JOURNAL OF VIROLOGY, Jan. 2003, p. 560–570 Vol. 77, No. 1
0022-538X/03/$08.00+0 DOI: 10.1128/JVI.77.1.560–570.2003

Concordant Modulation of Neutralization Resistance and High Infectivity of the Primary Human Immunodeficiency Virus Type 1 MN Strain and Definition of a Potential gp41 Binding Site in gp120

Maria Leavitt,[1]* Eun Ju Park,[1]† Igor A. Sidorov,[2] Dimiter S. Dimitrov,[2] and Gerald V. Quinnan, Jr.[1]

Uniformed Services University of the Health Sciences, Bethesda,[1] and Frederick Cancer Research Facility, National Cancer Institute, Frederick,[2] Maryland

Received 14 June 2002/Accepted 24 September 2002

Efforts to develop a vaccine against human immunodeficiency virus type 1 (HIV-1) are complicated by resistance of virus to neutralization. The neutralization resistance phenotype of HIV-1 has been linked to high infectivity. We studied the mechanisms determining this phenotype using clones of the T-cell-line-adapted (TCLA) MN strain (MN-TCLA) and the neutralization-resistant, primary MN strain (MN-P). Mutations in the amino- and carboxy-terminal halves of gp120 and the carboxy terminus of gp41 contributed to the neutralization resistance, high-infectivity phenotype but depended upon sequences in the leucine zipper (LZ) domain of gp41. Among 23 clones constructed to map the contributing mutations, there was a very strong correlation between infectivity and neutralization resistance ($R^2 = 0.81$; $P < 0.0001$). Mutations that distinguished the gp120s of MN-P and MN-TCLA clones were clustered in or near the CD4 and coreceptor binding sites and in regions distant from those binding sites. To test the hypothesis that some of these distant mutations may interact with gp41, we determined which of them contributed to high infectivity and whether those mutations modulated gp120-gp41 association in the context of MN-P LZ sequences. In one clone, six mutations in the amino terminus of gp120, at least four of which clustered closely on the inner domain, modulated infectivity. This clone had a gp120-gp41 association phenotype like MN-P: in comparison to MN-TCLA, spontaneous dissociation was low, and dissociation induced by soluble CD4 binding was high. These results identify a region of the gp120 inner domain that may be a binding site for gp41. Our studies clarify mechanisms of primary virus neutralization resistance.

The induction of a broadly protective neutralizing antibody response is a major concern regarding the potential efficacy of vaccines. Efforts to develop a vaccine against human immunodeficiency virus type 1 (HIV-1) have been slow as a result of resistance of virus to neutralization and difficulties in preparing envelope protein in a stable conformation that expresses conserved neutralization epitopes. This resistance is manifested in comparisons of primary virus isolates to laboratory-adapted viruses and antigenic variations among strains (2, 3, 17, 23). In some lentivirus infections, disease episodes occur intermittently and may be related to periods of increased viral replication that may follow occurrence of escape mutations (19). In HIV infection there is evidence of partial immune control of viral replication. Virus is readily detected in plasma early during acute infection, but at lower levels during the pre-AIDS period of chronic infection (38). Despite the partial control of replication, substantial virus replication remains ongoing during the chronic, pre-AIDS period of infection, with the potential for mutant strains to emerge (14, 36). Neutralization escape mutations may be important during the period of chronic infection or as an event contributing to late immunological deterioration.

Limited studies have been performed of neutralization escape mutations occurring in vivo or in vitro in the presence of sera from infected people or animals (27, 34). Evidence of V3 region escape mutation occurring early during the course of infection has been reported (32). Others have reported mutations at sites distant from neutralization epitopes, in gp41, that mediate a global resistance phenotype affecting neutralization by antibodies against multiple epitopes (2, 24, 26, 28, 37, 44). It has been considered likely that these mutations contribute to neutralization resistance through effects on conformation of the envelope complex.

The determination of the atomic structure of gp120 and the discovery that chemokine receptors are coreceptors for HIV have substantially advanced understanding of the nature of neutralization epitopes on the envelope complex and the potential role of these epitopes in cell attachment and entry (1, 8, 9, 19, 43). The neutralization epitopes that are functional on primary envelopes tend to be conformation dependent (9, 16, 40). Accessibility of some of the epitopes depends on conformational changes that occur after engagement of CD4 (39, 40). These CD4-induced epitopes are generally thought to be epitopes in the coreceptor binding site. As a result of poor neutralizing antibody responses to experimental vaccines, interest has developed in defining methods to induce antibodies

* Corresponding author. Mailing address: Department of Preventive Medicine and Biometrics, Uniformed Services University of the Health Sciences, 4301 Jones Bridge Rd., Bethesda, MD 20814. Phone: (301) 295-9782. Fax: (301) 295-1971. E-mail: mleavitt@usuhs.mil.
† Present address: 2337 Bentley Ct., Castro Valley, CA 94546.

against epitopes exposed during the conformational changes that follow receptor engagement. Characterization of the mechanisms of neutralization resistance and of target epitopes that may be functional in neutralization of primary isolates may substantially facilitate efforts to immunize effectively against HIV.

Previous studies involved the neutralization-sensitive, T-cell-line-adapted (TCLA), MN strain (MN-TCLA) strain and a clone derived from it, designated E6, by in vitro selection with a highly neutralizing human serum (33–35). The neutralization-resistant mutant phenotype of MN-E6 was attributable to two mutations in gp120 and four mutations in the leucine zipper (LZ) structure of gp41. The neutralization-resistant phenotype was found to be associated with a high-infectivity phenotype, which was attributable to five of the six mutations. The high infectivity is, in turn, probably the result of a number of steps leading to a very high efficiency of virus-cell membrane fusion (33). Here we report additional studies on the mechanisms of these phenotypes. Clones were studied that were developed previously from the extremely neutralization-sensitive MN-TCLA strain and the neutralization-resistant, primary MN strain (MN-P) of HIV-1. The studies demonstrated that the phenotypes were dependent upon multiple mutations distributed throughout gp120 and gp41 and functional interactions of regions of gp120 and gp41 with LZ sequences in gp41. Some of the mutations localize in or near gp120 binding sites for CD4 or coreceptor, while results presented here suggest that some other mutations may lie within a gp41 binding site. The neutralization resistance of the primary HIV-1 strain appears to be the result of multiple mutations that transduce effects throughout the envelope protein complex, conferring a high infection efficiency phenotype.

MATERIALS AND METHODS

Pseudotyped virus construction, infectivity titration, and neutralization assays. Viruses pseudotyped with envelope glycoproteins derived from various *env* plasmids were constructed using pSV7d-*env* and pNL-Luc-E-R-, as described previously (5, 33–35). The *env* plasmid DNA and pNL-Luc-E-R- were introduced into 50% confluent 293T cells by calcium phosphate transfection (Promega, Madison, Wis.). The culture medium was replaced with fresh medium containing 1 μM sodium butyrate at 18 h posttransfection. At 48 h after transfection, the pseudotyped-virus-containing supernatants were harvested, filtered through 45-μm-pore-size filters, and used immediately for infectivity and neutralization assays. Alternatively, filtered pseudotyped viruses, supplemented with additional fetal bovine serum to a final concentration of 20%, were stored at −80°C. To measure the infectivity of pseudotyped viruses, a luminescence assay with HOS $CD4^+$-$CXCR4^+$ cells was used. Cells (1.5×10^4/ml) were inoculated with serially diluted pseudotyped virus in 96-well plates with U-bottom wells. The cultures were incubated for 3 days at 37°C, after which the cells were washed with cold phosphate-buffered saline (PBS) and lysed with 15 μl of lysis buffer (Promega). Luciferase activity was read in a Luminoscan luminometer (Labsystem, Inc., Needham, Mass.). Relative infectivity was determined as $X_M/X_{\text{MN-TCLA}}$ (calculated using Microsoft Excel), where X is the virus dilution that yields a given activity, X_M is the value obtained for the particular mutant studied, and $X_{\text{MN-TCLA}}$ is the value obtained for MN-TCLA. Best-fit lines were determined by regression analysis of the log-transformed luciferase activity determinations (light units) as a function of inoculum dilutions. y values used for comparisons of MN-TCLA and other clones were selected so as to intersect approximately linear segments of the curves being compared. The neutralization phenotype of each pseudotyped virus was tested in a manner similar to that of the infectivity assay, except that 25-μl aliquots of serially diluted sera were mixed with equal volumes of the appropriate pseudotyped viruses and incubated for 1 h at 4°C, after which HOS $CD4^+$-$CXCR4^+$ cells were added. The pseudotyped-virus dilutions were selected to produce luminescence in the presence of nonimmune serum of about 100 times the background. The neutralization endpoints were considered to be the highest serum dilution calculated to cause a reduction of luminescence by 90% compared to the nonneutralized control. Human neutralizing serum 2 (HNS2) and the negative reference serum were used as reference neutralizing and nonneutralizing sera, respectively (catalog no. 1983 and 2411; NIH AIDS Research and Reference Reagent Program) (41).

Construction of chimeric envelope glycoprotein genes. The MN-TCLA and MN-P genes used in this study have been described previously (33, 34, 45). All amino acid residue numbers noted in this report correspond to the residue numbers for the clone MN-P. In some cases, these numbers differ from those described previously for MN-TCLA-derived clones. Several chimeric *env* clones were constructed by exchanging fragments of the neutralization-sensitive, MN-TCLA and the neutralization-resistant, MN-P parental *env* clones, as previously described (35). All chimeric *env* genes cloned into the pSV7d vector were sequenced by the ABI PRISM Big Dye-Terminator method (model 3100 genetic analyzer; Applied Biosystems, Foster City, Calif.). Analyses were performed using the EditSeq and MegAlign programs (DNASTAR Inc., Madison, Wis.). The specific restriction enzymes and the locations of their recognition sequences are shown in Fig. 2. The nucleotide positions are numbered based on the MNCG sequence (12). Chimeras A and B were constructed by digesting the plasmids with *Eco*RI (upstream of the *env* start codon in pSV7d) and *Sac*I (nucleotide [nt] 1550). Chimera A contains the entire sequence of gp120 from MN-TCLA with the rest of the region (gp41) from MN-P, since the *Sac*I site is located 4 amino acids downstream from the cleavage site between gp120 and gp41. Chimeras C, D, E, and F were constructed by initially subcloning the *Sac*I-*Sal*I fragments (725 bp) at nt 1550 and 2275 of both MN-TCLA and MN-P into pUC19. The products were called pUC19/MN-TCLA*env* and pUC19/P37*env*, respectively. To make chimera C, the *Sac*I-*Bsm*I fragment (267 bp) of pUC19/P37*env* was ligated with the *Bsm*I-*Sac*I fragment of pUC19/MN-TCLA*env*. The product was called pUC19/*env*C. The *Sac*I-*Sal*I fragment (725 bp) of pUC19/*env*C was then ligated with the large *Sac*I-*Sal*I fragment of MN-TCLA (4,493 bp). To make chimera D, the *Sac*I-*Bsm*I fragment (267 bp) of pUC19/MN-TCLA*env* was ligated with the *Bsm*I-*Sac*I fragment of pUC19/P37*env*. The product was called pUC19/*env*D. The *Sac*I-*Sal*I fragment (725 bp) of pUC19/*env*D was then ligated with the large *Sac*I-*Sal*I fragment of MN-TCLA (4,493 bp). To make chimera E, the *Sac*I-*Sal*I fragment (725 bp) of pUC19/*env*D was ligated with the large *Sac*I-*Sal*I fragment of MN-P (4,514 bp). To make chimera F, the *Sac*I-*Sal*I fragment (725 bp) of pUC19/*env*D was ligated with the large *Sac*I-*Sal*I fragment of MN-P (4,514 bp). Chimeras G and H were constructed by exchanging large and small *Bgl*II-*Bgl*II fragments of 571 and 4,668 bp, respectively, between MN-P and MN-TCLA. To construct chimera GC, the *Sac*I-*Sal*I fragment (725 bp) of chimera C was ligated with a large *Sac*I-*Sal*I fragment of chimera G (4,493 bp). To make chimera GD, the *Sac*I-*Sal*I fragment (725 bp) of chimera D was ligated with a large *Sac*I-*Sal*I fragment of chimera H (4,493 bp). To make chimera HC, the *Sac*I-*Sal*I fragment (725 bp) of chimera C was ligated with a large *Sac*I-*Sal*I fragment of chimera H (4,514 bp). Chimera HD was made by ligating a *Sac*I-*Sal*I fragment (725 bp) of chimera D with a large *Sac*I-*Sal*I fragment of chimera H (4,514 bp). Chimera I was constructed by ligating a *Bam*HI-*Bsu*36I fragment (1,324 bp) of chimera GD with a large *Bsu*36I-*Bam*HI fragment of MN-TCLA (3,894 bp). To make chimera J, a *Bsu*36I-*Sal*I fragment (1,175 bp) of chimera B was ligated with a large *Sal*I-*Bsu*36I fragment of MN-TCLA (4,043 bp). To make chimera K, a *Sac*I-*Sal*I fragment (725 bp) of chimera C was ligated with a large *Sal*I-*Sac*I fragment of chimera I (4,493 bp). To make chimera L, a *Sac*I-*Sal*I fragment (725 bp) of chimera C was ligated with a large *Sal*I-*Sac*I fragment of chimera J (4,493 bp). Chimera M was constructed by ligating a *Sac*I-*Sal*I fragment (725 bp) of chimera D with a large *Sal*I-*Sac*I fragment of chimera I (4,493 bp). To make chimera N, a *Sac*I-*Sal*I fragment (725 bp) of chimera D was ligated with a large *Sal*I-*Sac*I fragment of chimera J (4,493 bp).

The following eight chimeras were constructed to study possible gp120-gp41 interactions. To construct chimera O, a *Bam*HI-*Dra*III fragment (592 bp) of MN-P was ligated with a large *Dra*III-*Bam*HI fragment of chimera C (4,626 bp). To make chimera P, chimera H was first mutagenized to introduce an *Eco*RV site at nt 636, forming chimera H. The *Dra*III-*Eco*RV fragment (268 bp) of chimera H (plus *Eco*RV) was then ligated with a large *Eco*RV-*Dra*III fragment of chimera C (4,950 bp). To make chimera Q, the *Eco*RV-*Sac*I fragment (914 bp) of chimera H (plus *Eco*RV) was ligated with a large *Sac*I-*Eco*RV fragment of chimera C (4,304 bp). This clone was called Qa. The *Eco*RV site on Qa was then deleted to complete construction of chimera Q. To make chimera R, chimera Q was first mutagenized to introduce an *Eco*RV site at nt 636. The *Bam*HI-*Eco*RV fragment (636 bp) of chimera O (plus *Eco*RV) was ligated with a large *Bam*HI-*Eco*RV fragment of chimera Q (4,577 bp). Finally, the *Eco*RV site was mutagenized back to the chimera Q sequence at nt 636 to complete construction of chimera R. Chimera S was constructed by first mutating chimera C to introduce the four mutations N/K 300, S/R 345, S/P 398, and S/N 418. Then the *Bgl*II-*Bgl*II

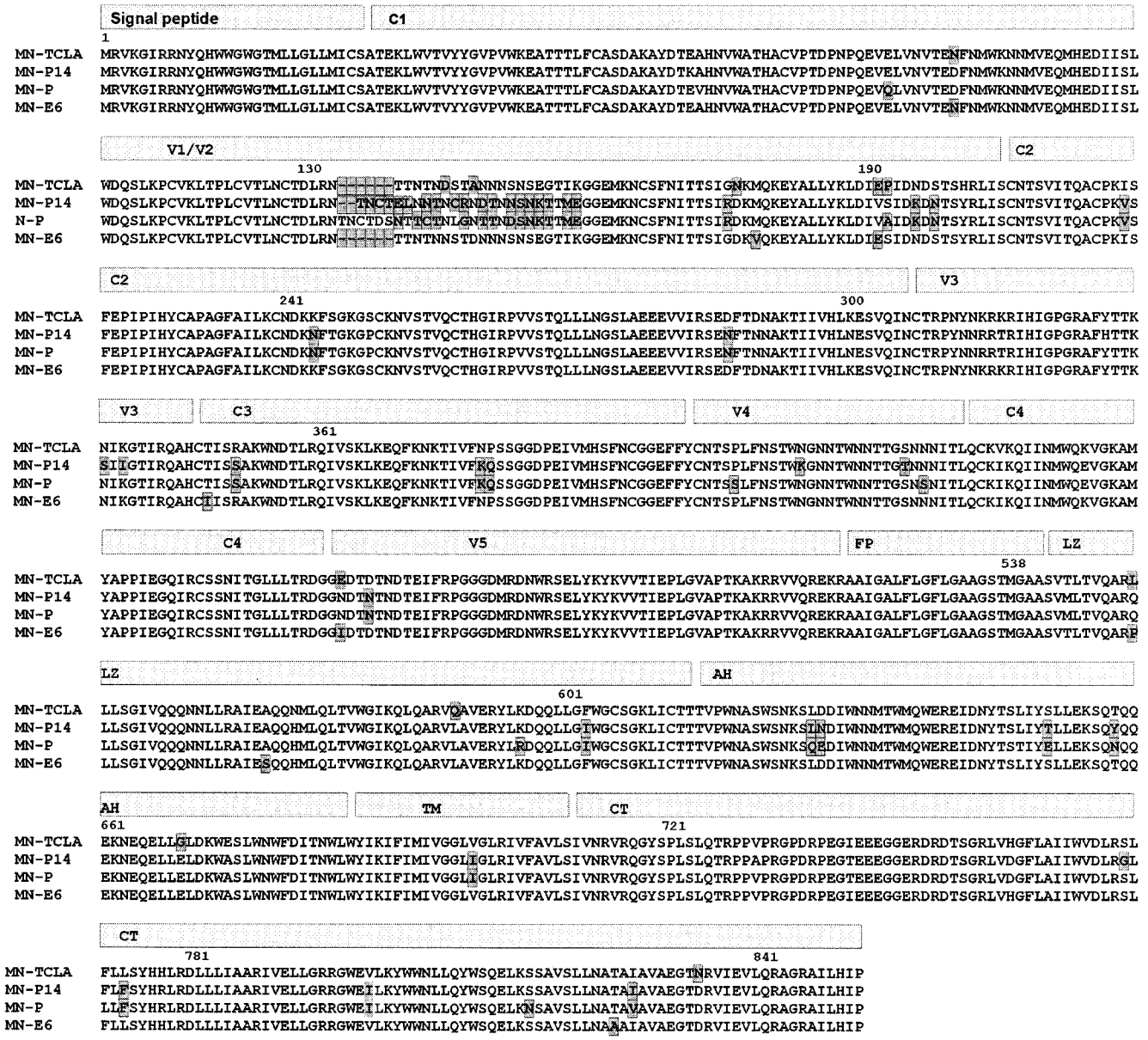

FIG. 1. Alignment of amino acid sequences of envelopes of neutralization-sensitive (MN-TCLA), highly neutralization-resistant (MN-P and MN-P14), and partially neutralization-resistant (MN-E6) clones of the HIV-1 MN strain. The bars above the amino acid sequences indicate the approximate locations of regions of the glycoproteins, as follows: C1, C2, C3, and C4, constant regions of gp120; V1/V2, V3, V4, and V5, variable regions of gp120; gp41 regions, fusion peptide (FP), LZ, AH (membrane proximal), TM, and CT. Positions of amino acids are numbered as in MN-P, and amino acids differing from consensus are boxed and shaded. Residues numbers appear in the boxes at locations corresponding to restriction enzyme cleavage sites illustrated in Fig. 2.

fragment (571 bp) of chimera C containing the four mutations was ligated with a large *Bgl*II-*Bgl*II fragment of chimera R (4,642 bp). The same *Bgl*II-*Bgl*II fragment (571 bp) of chimera C containing the four mutations was also ligated with a large *Bgl*II-*Bgl*II fragment of MN-TCLA (4,642 bp) to make chimera T. To make chimera U, the *Bam*HI-*Dra*III fragment (368 bp) of MN-P was ligated with a large *Bam*HI-*Dra*III fragment of MN-TCLA (4,845 bp). To make chimera V, the *Bam*HI-*Sac*I fragment (1,550 bp) of chimera R was ligated with a large *Bam*HI-*Sac*I fragment of MN-TCLA (3,663 bp).

Site-directed mutagenesis. Mutagenesis procedures were carried out using *Pfu* polymerase (QuikChange mutagenesis kit; Stratagene, La Jolla, Calif.) by following the instructions of the manufacturer. The reactions were performed in an automated thermal cycler (model 2400; Perkin-Elmer, Foster City, Calif.). Nucleotide sequences were confirmed by sequencing using the ABI PRISM Big Dye-Terminator method (model 3100 genetic analyzer; Applied Biosystems).

gp120 dissociation assay and ELISA. Spontaneous and ligand-induced gp120 dissociation was assessed by enzyme-linked immunosorbent assay (ELISA). Briefly, pseudotyped viruses in transfected cell culture supernatants were filtered, sedimented by centrifugation at 21,130 × *g* for 2 h at 4°C (Tomy Tech USA, Inc., Palo Alto, Calif.), washed once with prechilled PBS by centrifugation, and resuspended in PBS with 10% fetal bovine serum in 1/40 of the initial volume. We have previously reported that similar results are obtained when pseudotyped viruses are sedimented as pellets or onto a sucrose cushion and then into pellets (33, 34). Each aliquot of concentrated pseudotyped virus was incubated at 37°C for 1 h with a 5-μg/ml concentration of soluble CD4 (sCD4) or PBS. The pseudotyped particles were then separated from dissociated gp120 by centrifugation at 21,130 × *g* for 2 h. The level of gp120 dissociation was determined by comparing gp120 antigen levels in the samples of the supernatants and pellets measured by ELISA. The amounts of p24 antigen in both supernatant and

pellet samples were also measured. The ELISA was conducted by antigen capture, as described previously (33, 34). Briefly, each well of the microtiter plate (Immulon 2; Dynex Technology Inc., Chantilly, Va.) was coated with a human anti-HIV-1 immunoglobulin G; the antigen prepared in lysis buffer and diluted in blocking reagent was applied, and bound antigen was detected using either sheep anti-gp120 or rabbit anti-p24 antibody. Bound detection antibodies were assayed using biotinylated anti-sheep (Vector Laboratories, Inc., Burlingame, Calif.) or anti-rabbit antibody, followed by avidin-conjugated horseradish peroxidase (Vector Laboratories), and then orthophenylenediamine (Abbott Diagnostics Labs, North Chicago, Ill.) or TMB (Kirkegaard and Perry Laboratories, Gaithersburg, Md.) substrate development, respectively. Standard antigen controls used in the assays consisted of serial dilutions of p24 and MN strain gp120, each obtained from the NIH AIDS Research and Reference Reagent Program (catalog no. 382 and 3927, respectively).

Location of gp120 core mutation in the gp120 atomic structure. The PDF file used for the gp120 atomic structure is from the Protein Data Bank, 1GC1 (21) and was drawn with PC Molecule 2 (version 2.0.0; Molecular Ventures, Inc.). Figures representing the location of the mutations were drawn with PCMolecule2 (version 2.0.0; Molecular Ventures, Inc.) and with Corel Draw (version 8.369).

RESULTS

Nucleotide and amino acid sequences of primary MN clones. Two clones derived from the primary MN virus pool were selected based on being functional in infectivity assays when pseudotyped on virus particles. These clones are designated MN-P and MN-P14. The nucleotide sequences of these *env* genes were determined, and the predicted amino acid sequences were compared to those of the MN-TCLA and MN-E6 clones, described previously, as shown in Fig. 1 (33–35, 47). The MN-TCLA and MN-E6 clones were 98% similar to each other, but only 91.5 to 92.5% similar to the MN-P and MN-P14 clones. The MN-P and MN-P14 clones were 95.6% similar to each other. Among 88 amino acid residues at which the MN-P or MN-P14 clones differed from the MN-TCLA clone, the MN-P and MN-P14 clones both varied at 64 residues. Additionally, both the MN-P and MN-P14 clones had unusual insertional mutations in variable region 1 (V1 region) that resulted in two extra cysteine residues with probable formation of an extra disulfide bond. In both cases, it appeared that this insertion mutation had resulted from a duplication mutation. Thus, the MN-P clone was similar to the MN-P14 clone and is reasonably likely to be representative in the same sense of other clones that were present in the virus quasispecies mixture from which they were derived. Polymorphisms found while comparing highly neutralization-resistant MN-P and neutralization-sensitive MN-TCLA clones in gp120 include three in the constant region 1 (C1 region), seven in the V1/V2 region, seven in the C2 region, four in the V3 region, three in the C3 region, two in the V4 region, two in the C4 region, and two in the V5 region. The polymorphisms in gp41 included seven in the amino-terminal segment of gp41 proximal to the disulfide-bonded loop (most or all of this region is alpha-helical [AH] in structure in the fusion active state, and the region will be subsequently referred to in this paper as the LZ domain), seven in the membrane proximal AH region, one in the transmembrane segment (TM), and nine in the cytoplasmic tail (CT).

The MN-P clone differed from MN-TCLA at five of the six residues at which mutations have been previously reported as causing the differences in neutralization resistance phenotypes of MN-E6 and MN-TCLA (33). At three of these residues the mutations that distinguished MN-P and MN-E6 from MN-TCLA were the same: I/V 426, H/N 571, and L/Q 588. The respective amino acids at residue 466 were N, E, and I, and those at residue 550 were Q, L, and P, for clones MN-P, MN-TCLA, and MN-E6. Thus, MN-E6 may have been derived from a clone in a quasispecies mixture that was a common ancestor to the MN-P clone and had persisted in the MN-TCLA virus pool.

Neutralization resistance and high-infectivity phenotypes of MN-P. The neutralization sensitivity and infectivity of the MN-P and MN-TCLA clones and various chimeric genes derived from them are presented in Fig. 2. The infectivity and neutralization results shown are the mean results of eight comparative tests of the MN-TCLA and MN-P clones. The results shown for each of the other clones shown are the mean result for three to five tests per clone; each one of these tests was included in one of the experiments shown comparing the MN-TCLA and MN-P clones. In addition, each of the clones regarding which direct comparisons are made in this section was included in repeated experiments in which they were compared directly. The MN-P clone was 1,250-fold more infectious in HOS $CD4^+$-$CCR5^+$ cells than the MN-TCLA clone and 256-fold more resistant to neutralization by the reference serum HNS2. The neutralization resistance and infectivity of MN-P are similar to those characteristics of other primary HIV-1 envelopes that have been tested in our laboratory (45, 46). The chimeric clones were constructed to permit evaluation of regions of the MN-P gene responsible for the high-infectivity and neutralization resistance phenotypes of MN-P. Chimera A derived its 5′ sequences, up to the *Sac*I site, located four codons downstream of the coding sequence for the gp120-gp41 cleavage site, from MN-TCLA and derived its 3′ sequences from MN-P. It was consistently intermediate in infectivity and neutralization resistance in comparison to MN-P and MN-TCLA. Chimera B derived its 5′ sequences, up to the *Sac*I site, from MN-P and derived its 3′ sequences from MN-TCLA. It was less infectious and resistant to neutralization than chimera A but slightly more infectious and neutralization resistant than MN-TCLA. These results indicate that sequences in both gp120 and gp41 contribute to the high-infectivity, neutralization resistance phenotype of MN-P.

Previous studies reported from this laboratory demonstrated that the high-infectivity, neutralization resistance phenotype of the MN-E6 clone was attributable to functional interactions between the carboxy-terminal region of gp120 and the LZ region of gp41. Chimeras C and F were constructed to permit testing of the importance of the LZ region of MN-P. Chimera C, which was constructed by the introduction of the LZ region of MN-P into MN-TCLA, had slightly increased neutralization resistance and infectivity compared to MN-TCLA. Conversely, chimera F, which consisted of mostly MN-P sequences with the LZ region derived from MN-TCLA, was also only slightly more infectious and neutralization resistant than MN-TCLA. These results demonstrated that the high-infectivity, neutralization resistance phenotype of MN-P was dependent upon the LZ sequence, but this sequence was not sufficient to impart the phenotype.

The functional interaction of the amino terminus of gp120 with LZ sequences was evaluated by comparison of chimeras C, F, HC, and HD. Chimera HC incorporated sequences from

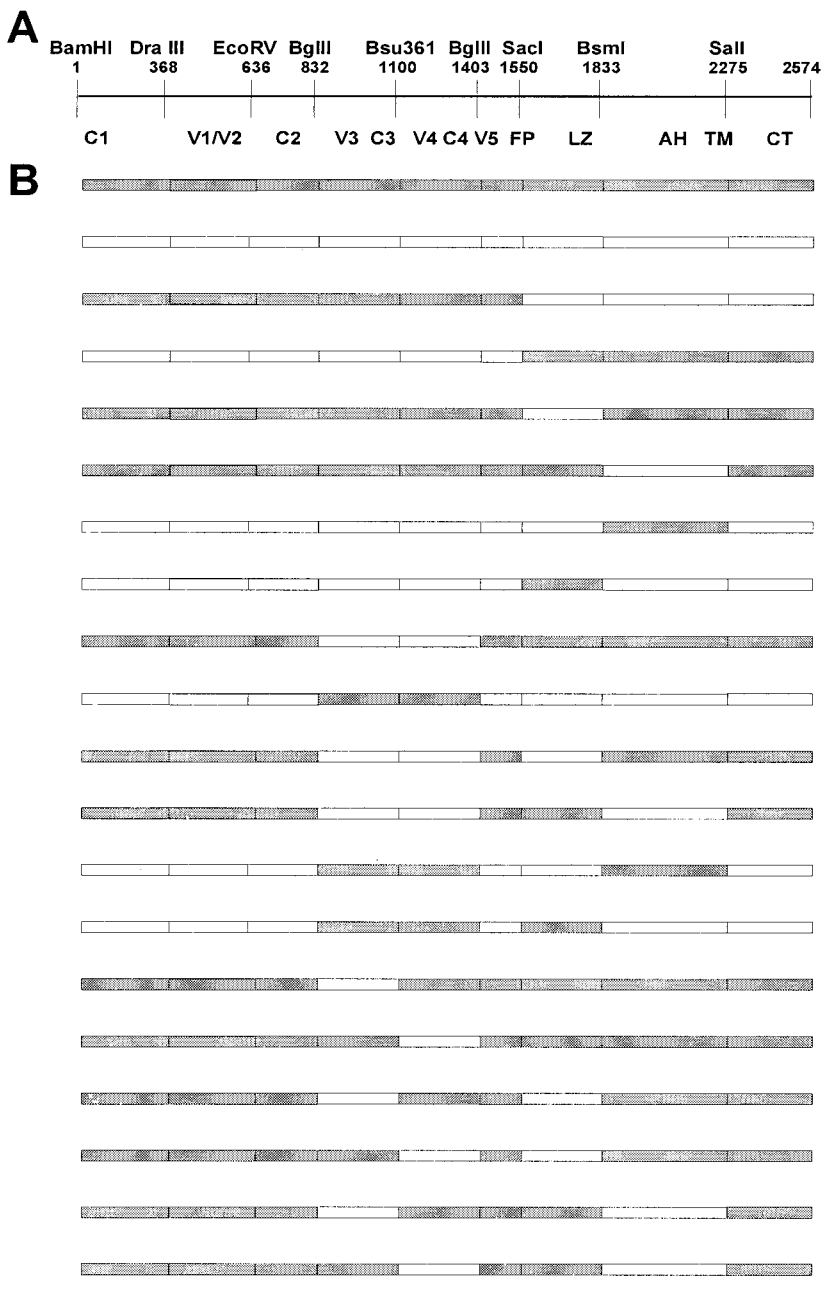

C

Clone	Relative Infectivity	1/Neut. Titer
MN-TCLA	1	4096
MN-P	1215	16
Chim A	128	256
Chim B	8	1024
Chim C	4	1024
Chim D	1.25	4096
Chim E	256	32
Chim F	8	1024
Chim G	1.5	1024
Chim H	64	64
Chim GC	128	32
Chim GD	1	2048
Chim HC	96	256
Chim HD	1.5	2048
Chim I	1	2048
Chim J	1	4096
Chim K	8	512
Chim L	64	512
Chim M	0.5	4096
Chim N	0.5	4096

FIG. 2. The gp41 LZ interacts functionally with multiple regions of gp120 and gp41 to determine the neutralization resistance, high-infectivity phenotype. (A) Restriction endonuclease cleavage map of the MN-TCLA clone indicating nucleotide positions of cleavage sites for specific enzymes. Below the map are indications of the approximate locations of regions of the glycoproteins, as follows: C1, C2, C3, and C4, constant regions of gp120; V1/V2, V3, V4, and V5, variable regions of gp120; gp41 regions, fusion peptide (FP), LZ, AH (membrane proximal), TM, and CT. (B) Schematic description of a series of chimeric genes (Chim) constructed by exchanging segments of the MN-TCLA and MN-P clones, as described in Materials and Methods. (C) Relative infectivity and neutralization (Neut.) titers obtained for the clones. Relative infectivity was determined as $X_M/X_{\text{MN-TCLA}}$ (calculated using Excel), where X is the virus dilution that yields a given activity, X_M is the value obtained for the particular mutant studied, and $X_{\text{MN-TCLA}}$ is the value obtained for MN-TCLA. Best-fit lines were determined by regression analysis of the log-transformed luciferase activity determinations (light units) as a function of inoculum dilutions. y values used for comparisons of MN-TCLA and other clones were selected so as to intersect approximately linear segments of the curves being compared. Neutralization phenotypes of chimeras were determined by using HIV HNS2. Titers are the reciprocal serum dilutions resulting in ≥90% inhibition of infectivity. Each chimeric clone was tested three to five times in comparison to MN-P and MN-TCLA, and geometric mean results are presented.

the amino terminus of MN-P gp120 and the amino terminus and cytoplasmic tail of MN-P gp41 into the MN-TCLA background. Chimera HC was substantially more infectious and neutralization resistant than chimera C or F. It is likely that these phenotypic characteristics of chimera HC reflect functional interactions between the amino terminus of gp120 and the LZ region of gp41. These results extended the scope of functional interactions previously described and responsible

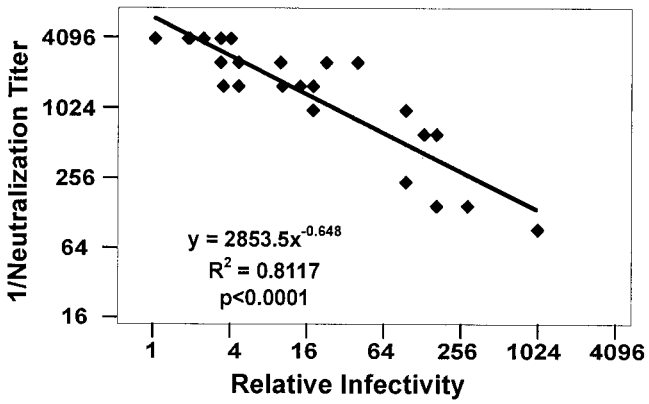

FIG. 3. Correlation between neutralization resistance and infectivity of viruses pseudotyped with mutant and chimeric MN strain envelope clones. Data shown in Fig. 1 were analyzed in Excel. The null hypothesis of no correlation was rejected with a P of <0.0001.

for the differences in neutralization resistance phenotypes of MN-E6 and MN-TCLA, where only two mutations in the carboxy-terminal half of gp120 interacted with the LZ region of gp41. The possibility that the cytoplasmic domain of gp41 could contribute to some of the phenotypic effects as suggested by Edwards et al. (7) remains to be determined.

The possibility of functional interaction between the carboxy terminus of gp120 and the LZ region is indicated by comparison of chimeras C, G, H, and GC. There were relatively small differences between chimera G and MN-TCLA, while chimera GC was substantially more infectious and neutralization resistant. These comparisons indicate that the relatively high-infectivity, neutralization resistance phenotype of chimera GC is probably due to functional interactions between the carboxy terminus of gp120 and the LZ. Results of testing of chimeras I, J, K, L, M, and N further support the interpretation that functional interactions occur between different regions of the carboxy terminus of MN-P gp120 and the LZ, contributing to the neutralization resistance, high-infectivity phenotype.

We questioned whether the MN-P LZ was contributing to the phenotype by interaction with other regions of gp41. Comparisons of chimeras A, C, D, GD, E, and HD indicated a probable functional interaction of the AH region of gp41 with the LZ region. Chimera A contains sequences of the entire MN-P gp41 and was substantially more infectious and neutralization resistant than either chimera C or D. Chimera D contained the MN-P sequences encoding the AH of the gp41 ectodomain. Conversely, chimera E had MN-P sequences throughout, except for the AH region, and it was significantly less infectious than MN-P. Chimeras GD and HD combined MN-P AH sequences with sequences from other regions of MN-P, excluding the LZ region, and no complementation was observed. These results indicate a specific functional interaction between the LZ and AH regions, contributing to the neutralization resistance, high-infectivity phenotype of MN-P.

Based on the analyses presented here, the results presented in Fig. 2 demonstrate probable functional interactions of the MN-P LZ region with the amino and carboxy termini of gp120 and the AH region of gp41. These results thus extend the evidence described in our previous report, indicating that the

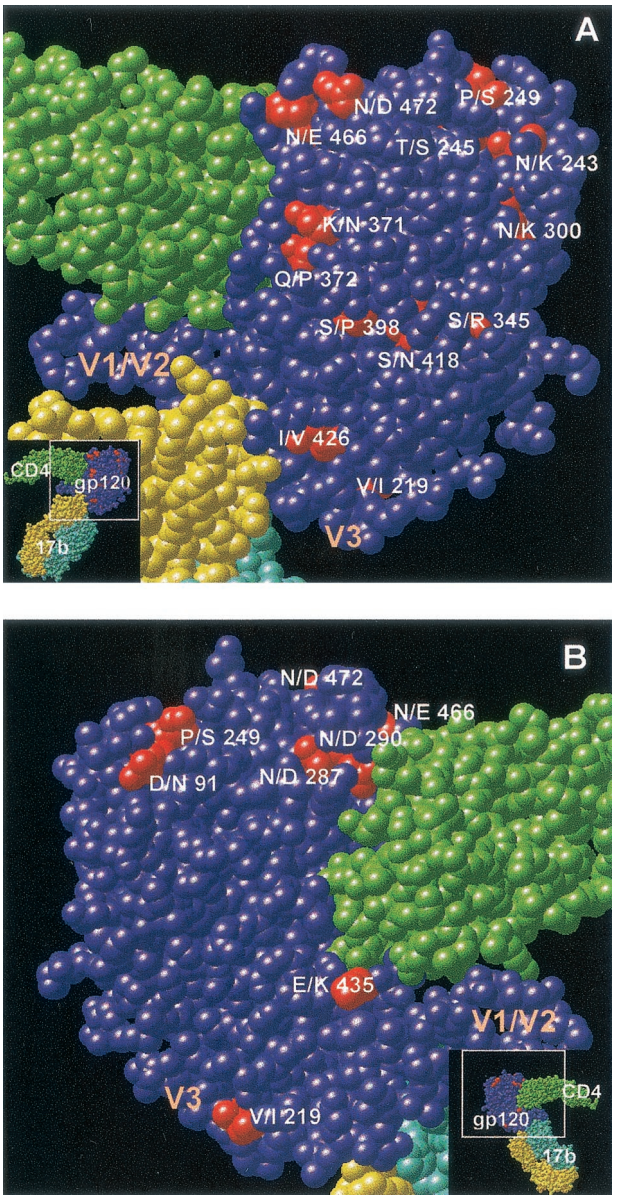

FIG. 4. Localization of MN-P/MN-TCLA mutations in the atomic structure of HIV-1 gp120 core complexed with CD4 and a neutralizing antibody, 17b. The PDF file is from the Protein Data Bank, 1GC1 (21) and drawn with PCMolecule2 (version 2.0.0; Molecular Ventures, Inc.). The front (A) and back (B) sides of the molecular complex are shown. The gp120 is shown in blue, CD4 is shown in green, and the 17b antibody is shown in yellow (light chain) and in pale blue (heavy chain). The amino acid sequence of gp120 was extracted from the PDF file and aligned with the sequence of MN-TCLA by Clustal W (version 1.7; National Institutes of Health). Mutation sites are colored red and marked as MN-P amino acid/MN-TCLA amino acid followed by the position number of each mutation in the MN-P sequence. Locations of V1/V2 and V3 loops are also indicated.

LZ region plays a significant role in organizing the functions of the HIV-1 envelope protein complex (33). Moreover, there was a general correspondence between effects of specific mutations on the two characteristics of the phenotype being evaluated. To test the possibility that these multiple functional interactions between the LZ and other regions of the envelope

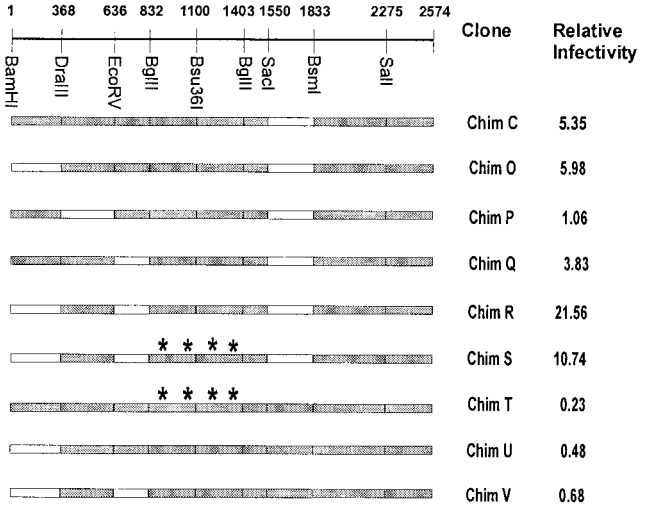

FIG. 5. Effects of inner-domain and selected outer-domain mutations on infectivity. The restriction enzyme cleavage map of MN-TCLA, shown at top, is described in the legend to Fig. 2. Schematic diagrams of chimeric *env* genes constructed using fragments of the MN-TCLA and MN-P genes are shown on the left. Stars above the diagrams of chimeras (Chim) indicate the approximate locations of mutations introduced in vitro (see text for description). Relative infectivities of viruses pseudotyped with envelopes encoded by the chimeric genes are shown to the right.

proteins were modulating both characteristics simultaneously by common mechanisms, we tested whether there was a statistical correlation between the characteristics, as shown in Fig. 3. A strong, statistically significant correlation was obtained.

Localization of MN-P mutations in the core of the atomic structure of gp120. The localization of mutations in the core structure of MN-P gp120 was examined, as illustrated in Fig. 4. Only those mutations affecting residues visualized in the gp120 core structure are shown. Mutations in the extreme amino-terminal first 90 amino acids and the V1/V2 and V3 regions of gp120 are not shown in the figure. Seven of the mutations were identified as being localized in or around the rim of the CD4 binding pocket. These seven mutations are shown as N/D 287, N/D 290, K/N 371, Q/P 372, E/K 435, N/E 466, and N/D 472. Two of the mutations are localized in the region of gp120 considered to be the coreceptor binding domain and are identified as V/I 219 and I/V 426. Four of the mutations are localized to the pole of gp120, described as the inner domain, including D/N 91, N/K 243, T/S 245, and P/S 249. Four mutations were localized in the outer-domain of gp120 but were distant from the CD4 or coreceptor binding sites. These four mutations were N/K 300, S/R 345, S/P 398, and S/N 418. The distributions of these mutations suggested to us the possibility that some or all of them functioned in aggregate to enhance the infectivity and neutralization resistance of MN-P by modulating the interactions of gp120 with its ligands, including CD4, coreceptor, and gp41. The remainder of this report describes studies that were conducted to test the hypothesis that some of the mutations found in the MN-P gp120 core structure contribute to the high-infectivity phenotype by altering interaction of gp120 with gp41.

Specific mutations distant from CD4 and coreceptor binding sites in the core of gp120 contributing to the high-infectivity phenotype of MN-P. Chimeric envelopes were constructed to evaluate the specific contributions of gp120 amino-terminal sequences, including V1/V2 sequences, to the neutralization resistance, high-infectivity phenotype. V1/V2 sequences are included in the *Dra*III368-*Eco*RV636 segment shown in Fig. 2. The potential contribution of the V1/V2 region mutations to phenotype was evaluated by comparison of chimeras C, HC, O, P, and Q (Fig. 2 and 5). The infectivity of clones O, P, and Q was similar to that of chimera C, indicating that sequences in more than one subsegment of the *Bam*HI-*Bgl*II (832 bp) segment are required to determine the phenotype of chimera HC.

We constructed chimera R for further study of the role of gp120 core structure mutations in the amino terminus in determining the infectivity phenotype. Chimera R includes all of the mutations in the *Bam*HI-*Bgl*II segment of MN-P, except those in the V1/V2 region. While chimera R was somewhat less infectious than chimera HC (Fig. 2), it was significantly more infectious than chimera C, O, or Q, indicating that the two segments in the amino-terminal region of gp120 functioned together, in the context of MN-PLZ sequences, to determine enhanced infectivity.

Chimera S was constructed by introducing the outer-domain core structure mutations not associated spatially with the CD4 or coreceptor binding sites into chimera R. Chimera S was less infectious than chimera R, indicating that the effect of the mutations in the non-V1/V2 segments of the amino terminus of MN-P gp120 on infectivity was not further enhanced by

TABLE 1. Sedimentation analysis of particle association of gp120 and p24 of various HIV-1 *env* genes

Ligand	Fraction	Mean antigen concn ± SEM determined by ELISA of[a]:							
		MN-TCLA		MN-P		Chimera R		Chimera V	
		gp120 (ng/ml)	p24 (μg/ml)	gp120 (ng/ml)	p24 (μg/ml)	gp120 (ng/ml)	p24 (μg/ml)	gp120 (ng/ml)	p24 (μg/ml)
None	P	6.4 ± 2.7	11.5 ± 2.6	25.3 ± 6.1	6.7 ± 2.4	25.2 ± 3.3	15.2 ± 2.8	11.2 ± 4.8	15.8 ± 2.2
	SN	2.9 ± 0.8	2.7 ± 1.3	2.9 ± 1.8	1.4 ± 0.6	6.2 ± 2.1	3.5 ± 1.8	5.2 ± 1.6	5.5 ± 1.4
sCD4	P	6.4 ± 3.0	12 ± 2.2	25.6 ± 5.8	6.6 ± 2.2	20.1 ± 3.4	15.4 ± 2.1	11.6 ± 4.3	15.3 ± 2.1
	SN	2.9 ± 1.0	2.6 ± 1.2	14.0 ± 4.2[b]	1.1 ± 0.5	15.0 ± 5.7	4.4 ± 1.9	5.5 ± 1.8	6.1 ± 2.0

[a] Amount of gp120 and p24 in pellets (P) and supernatants (SN) of centrifuged suspensions of viruses pseudotyped with each envelope with or without preexposure to sCD4. Centrifugation was for 2 h at 4°C and 21,130 × *g*. Viruses were preincubated with sCD4 at 5 μg/ml for 1 h at 37°C. gp120 and p24 antigen concentrations (means ± standard errors of the means) were determined by ELISA of MN-TCLA ($n = 5$), MN-P ($n = 5$), chimera R ($n = 3$) and chimera V ($n = 3$). All tests shown included MN-P for comparison to other clones.

[b] Mean value differs from that in the samples not preincubated with sCD4 at $P < 0.05$ (nonparametric, Wilcoxon signed rank test).

these outer-domain mutations. Results shown from testing of chimeras T, U, and V further support the interpretations presented in this section.

gp120-gp41 dissociation. Noncovalent bonding between residues of gp120 and gp41 maintains the association between the two molecules in the functional envelope protein complex. Because of our interest in the possibility that mutations in gp120 modulated the interaction between gp120 and gp41 in a way that contributed to the high-infectivity phenotype, we tested the effects of MN-P mutations on the stability of the gp120-gp41 association. Furthermore, since binding of gp120 to CD4 affects its association with gp41 in some cases and since our hypothesis was that concerted interactions between gp120 and its ligands determine its infectivity phenotype, we tested the effect of sCD4 binding on gp120-gp41 dissociation. To measure the dissociation of gp120 from gp41, we used ELISA to determine the separation of particle-free and particle-associated gp120 that resulted from centrifugation of pseudotyped virus particles. We have previously found that this technique of separating virus particles from medium supernatants by centrifugation of the particles into pellets yields results comparable to those obtained when particles are collected on sucrose cushions.

Experiments were conducted comparing the spontaneous and sCD4-induced dissociation of gp120 from gp41 for MN-TCLA, MN-P, and chimeras R and V. Chimera R contains all of the MN-P mutations localized to the inner domain of gp120 on the atomic structure of the molecule, as well as two mutations in the amino terminus of the MN-P gp120 that were not visualized by Kwong et al. (21), specifically, V/A 64 and Q/E 84. It also contains the MN-P LZ sequences. Chimera V contains the same gp120 MN-P sequences but contains the MN-TCLA LZ sequences. The results of experiments testing the dissociation of gp120 from these pseudotyped viruses are summarized in Table 1. The effectiveness of separation of particles from medium components was evaluated by determining the relative amounts of p24 in pellets and supernatants. The percentage of p24 in the supernatants averaged between 14.9% (MN-P plus sCD4) and 28.8% (chimera V plus sCD4). In each case, these proportions were similar in the presence and absence of sCD4.

The amount of gp120 measured in association with virus particles, in the absence of sCD4, was consistently greater for MN-P than for MN-TCLA (Table 1). This difference averaged approximately fourfold. The amount of gp120 associated with chimera R pellets was also greater than that associated with MN-TCLA pellets, by 3.9-fold. There was slightly more gp120 associated with chimera V than MN-TCLA particles, by 1.75-fold. Thus, chimera R resembled MN-P in the greater association of gp120 with viral particles, while chimera S was very similar to MN-TCLA. Normalization of the gp120 results based on amount of p24 per sample did not substantially alter these comparisons (results not shown).

Spontaneous dissociation of gp120 from MN-TCLA, in the absence of sCD4, was 31.2%, significantly greater than that from MN-P, which was 10.3%. Spontaneous gp120 dissociation of gp120 from chimera R was lower than that from MN-TCLA, 19.8%, while dissociation from chimera V was nearly identical to that from MN-TCLA, 31.8%. When bound by sCD4, there was no change in the release of gp120 from MN-TCLA, but gp120 release from MN-P increased more than threefold, to 35.3%. Binding by sCD4 significantly enhanced gp120 release from chimera R to 42.7% but had no significant effect on release from chimera V. Thus, chimera R also resembled MN-P with respect to spontaneous and sCD4-induced release of gp120 from virions, while chimera V closely resembled MN-TCLA in these respects.

DISCUSSION

In this report we describe a neutralization resistance, high-infectivity phenotype of the primary HIV-1 MN strain envelope, MN-P, and we define genetic bases and infer structure-function relationships responsible for this phenotype. The MN-P strain was similar to other primary envelopes and was much more neutralization resistant and infectious than strain MN-TCLA (46). The results of mapping studies using genes chimeric for various segments of the MN-P and MN-TCLA genes demonstrated that the two characteristics of the phenotype were dependent on sequences in the segment of gp41 encoding the LZ domain, extending from the fusion peptide to the conserved disulfide bond, and were determined by functional interactions between this region and the amino- and carboxy-terminal halves of gp120 and the carboxy-terminal segment of gp41. Although the mutations carried by these interacting segments were distributed throughout the MN-P gene, analysis of the core structure of gp120 suggested clustering of mutations near the CD4 and coreceptor binding sites. Additional mutations were located on a face of the protein distant from these sites, on the inner and outer domains of the molecule. Among a large group of mutant and chimeric genes there was a strong correlation between neutralization resistance and infectivity, suggesting that mutations in these various regions of gp120 and gp41 were interacting functionally in a concerted fashion to determine the two-part phenotype. We pursued the hypothesis that this concerted effect involved the interactions of gp120 with its ligands, CD4, coreceptor, and gp41. Accordingly, studies were conducted to evaluate mutations that might be involved in direct gp41 interaction. A group of mutations, at least four of which are closely associated in the inner domain of gp120, were found to determine a functional interaction with the LZ domain that resulted in enhanced infectivity. An envelope with these and two other mutations in the amino terminus of gp120 was found to have a gp120-gp41 dissociation phenotype that characterized MN-P and distinguished it from MN-TCLA. These results thus identify a potential gp41 binding site on gp120. Overall, the studies presented here demonstrate that HIV-1 neutralization resistance is due to multiple, coordinated structure-function relationships and functional interactions within the envelope protein complex.

The studies described in this report were carried out to extend studies of mechanisms of neutralization resistance reported previously from this laboratory (33–35). The previous studies involved the MN-TCLA strain and a clone derived from it, E6 (34, 35). The MN-E6 clone is about 10-fold more neutralization resistant and infectious than the MN-TCLA clone. This phenotype depends upon functional interactions between sequences in the LZ region of gp41 and residues near the CD4 and coreceptor binding domains of gp120 (both mu-

tations are in the carboxy-terminal half of gp120). These results were surprising in that the human serum used for selection had a high level of neutralizing activity directed at the V3 loop (33), and it had been anticipated that neutralization escape might occur as a result of mutation in V3. In fact, the results were consistent with other reports of neutralization resistance mutations that were not localized in known neutralization epitopes (2, 24, 26, 37, 44). The finding that the MN-P clone was about 100-fold more infectious and 25-fold more neutralization resistant than the partially resistant MN-E6 clone provided a potentially powerful model for further study of the previously reported phenomena. The MN-P clone that we selected for study was very similar to another clone of primary MN virus, the nucleotide sequence of which was also determined. The similarity extended to an unusual duplication in the V1/V2 region, indicating that the MN-P clone is reasonably likely to be representative of other envelope clones that were present in the donor of the MN virus. The MN-P clone differed from MN-TCLA by many more mutations than did MN-E6 (Fig. 1). Interestingly, however, the two residues at which mutations in MN-E6 gp120 contributed to its neutralization resistance and high infectivity (V420I and E460I, as numbered in the original report) were also mutated in MN-P (I/V 426 and N/E 466, as numbered in Fig. 1). Furthermore, we have previously described the neutralization resistance of the MN-P clone to monoclonal antibodies directed against multiple conformation-sensitive epitopes, in comparison to MN-TCLA and MN-E6 (35). Our studies of genes chimeric for MN-P and MN-TCLA sequences demonstrated that functional interaction of the LZ region of gp41 with residues in the carboxy terminus of gp120 was necessary, but not sufficient, for the neutralization resistance, high-infectivity phenotype, as it was in the case of E6. However, in the case of MN-P, the phenotype was dependent upon the functional interaction of the LZ not just with residues in the carboxy terminus of gp120 but also with the amino terminus of gp120 and the carboxy terminus of gp41 (Fig. 2). In addition, the correlation between infectivity and neutralization resistance found in comparison of clones related to MN-TCLA and E6, previously, was confirmed in the present studies by examination of a much larger number of clones in which the phenotypic characteristics covaried over much broader ranges (Fig. 3). We interpret these data as indicating that the functional interactions within the envelope protein complex that were found to determine the neutralization resistance, high-infectivity phenotype of MN-E6 are reflected in the greater array of functional interactions that determine the more substantial phenotype of MN-P.

In order to further identify possible structure-function relationships determining the phenotype of MN-P, we examined the localization of mutated residues in the core structure of gp120, as reported by Kwong et al. (21). Seventeen mutations distinguished this part of the envelope of MN-P from MN-TCLA (Fig. 4). Seven of these mutations were seen to be localized in or near the CD4 binding site, and two were located in the region considered to constitute a major part of the coreceptor binding site (V/I 219 and I/V 426). The remaining eight mutations were located distant from these two ligand binding sites. This distribution of mutations prompted the hypothesis on our part that the phenotype under study was determined by concerted effects of alterations in interaction of gp120 with its ligands, CD4, coreceptor, and gp41. We, therefore, conducted additional studies to examine the possibility that certain of these mutations distant from the CD4 and coreceptor binding sites might affect gp120-gp41 interactions.

The potential interactions of the gp120 core structure mutations distant from the CD4 and coreceptor binding sites with gp41 were examined by study of the mutations in two groups. Four of the mutations (D/N 91, N/K 243, T/S 245, and P/S 249, numbered as in Fig. 4) were located in the inner domain reported by Kwong et al. (21). The other four mutations (N/K 300, S/R 345, S/P 398, and S/N 418, numbered as in Fig. 4) were located in the outer domain of the core structure of gp120. The locations of the four inner-domain mutations were consistent with interpretations of Kwong et al., based on structural modeling, that this pole of the molecule is likely to be oriented toward the trimeric axis of the oligomer (22). The effects of these two groups of mutations on infectivity, when present in the context of MN-P LZ sequences, were examined. The four inner-domain mutations, plus two additional amino-terminal mutations not visualized in the crystallographic structure reported by Kwong et al., worked cooperatively to enhance infectivity in a manner that was dependent upon sequences from the MN-P LZ region. The other four mutations, located on the outer domain of gp120, did not enhance infectivity in the context of the MN-P LZ sequences (Fig. 5). These results raised the possibility the inner-domain and amino-terminal mutations altered the surface of gp120 that interacts directly with gp41. The involvement of the three most-amino-terminal mutations of these six (V/A 64, Q/E 84, and D/N 91 in Fig. 1) in formation of a gp41 binding site would be consistent with a previous report of Wyatt et al. (43). They found that gp41 occluded binding of antibodies to the nonneutralizing face of gp120 and that deletion of amino acid sequences through residue 93 influenced the accessibility of these epitopes. Previous reports have not implicated residues carboxyl to the V1/V2 region in gp41 binding (15). However, the localization of residues 243, 245, and 249 to the inner domain of the nonneutralizing face of gp120, as well as the close proximity of these residues to residue 91 on the core structure of gp120 (Fig. 4), is consistent with the possibility that these mutated residues may comprise part of a gp41 binding site.

Spontaneous loss of gp120 from the HIV-1 virion surface has been reported to occur over time (10, 11, 20, 30). Spontaneous gp120 shedding from resistant primary isolates of HIV-1 is less than that from TCLA isolates (13, 18). The noncovalent association of the gp120 and gp41 envelope glycoprotein is disrupted by sCD4 binding to gp120, with resultant shedding of gp120 from the virion surface (26, 29–31, 40) and gp41 exposure required for virus entrance (4, 6, 25). In our previous studies, functional interaction between residues 426 and 466 in the E6 clone gp120 and residues in gp41 did not affect stability of the gp120/gp41 complex of the neutralization-resistant mutant MN-E6 (33). By contrast, in the present study we found that MN-P and MN-TCLA differ substantially with respect to spontaneous and CD4-induced shedding of gp120 from gp41. In contrast to the pattern of spontaneous gp120 shedding, no response of MN-TCLA to sCD4 was detected in gp120-gp41 dissociation assays, but significant dissociation followed sCD4 interaction with MN-P. In these respects, MN-P displayed a primary virus phenotype, while MN-TCLA displayed a TCLA

virus phenotype. The chimera containing the six mutations discussed above as potentially contributing to the gp41 binding site plus the MN-P LZ sequences (chimera R [Fig. 5]), displayed the MN-P-like, primary virus gp120-gp41 dissociation phenotype, while the chimera containing the same gp120 sequences but the complete gp41 sequence from MN-TCLA (chimera V [Fig. 5]) displayed the TCLA virus shedding phenotype. These results further support the interpretation that the region of the gp120 inner domain demarcated by these residues may constitute the binding site on gp120 for gp41. Conversely, they also suggest that the gp41 LZ sequence comprises the binding site for gp120. Further, the association of these same mutations with a high-infectivity phenotype may indicate that the primary virus dissociation phenotype is a reflection of high-efficiency responsiveness to CD4 binding.

The evidence that we present showing that the LZ region coordinates with multiple regions of gp120 and gp41 to determine the neutralization resistance, high-infectivity phenotypes is notable. These results are consistent with the previous reports of Park et al. (33, 34) but extend the evidence for regions that interact functionally with the LZ to include the amino-terminal half of gp120 and the carboxy terminus of gp41. Direct interactions of the LZ with amino acid residues in the CD4 and coreceptor binding sites are not likely. However, it is possible that the site on gp120 that associates noncovalently with gp41 does actually bond to this heptad repeat structure. Structural studies indicate that noncovalent bonding between residues on the hydrophobic face of the LZ mediates oligomerization of the envelope (4, 42). Additional structural studies indicate that an alpha-helix formed by amino acid residues in the carboxy-terminal ectodomain of gp41 associates with the trimeric structure formed by association of LZ structures, forming a six-helix, coiled-coil structure (4). This six-member coiled-coil structure is thought to represent the fusion-active state of the molecule. The bonding of the carboxy-terminal alpha-helices to the LZ structures involves amino acids different from those that mediate oligomerization of the LZs. On the surface of this six-member coiled-coil there is a face of each LZ that is apparently not occupied by bonding to the other members of the structure, consisting generally of the so-called b, c, and f residues of the LZ heptad repeat. It was notable that the four mutations in LZ that distinguished MN-E6 from MN-TCLA in the LZ were all located on this "unoccupied face" of the LZ. Remarkably, the same is true of mutations in MN-P LZ that distinguish it from MN-TCLA. In the sequence that extends from the fusion peptide to the disulfide-bonded gp41 loop, six of the seven mutations would be predicted to occupy b, c, or f positions on the helical wheel. Moreover, three of the four residues that were mutated in MN-E6 were also mutated in MN-P. These observations indicate the possibility that the LZ may bond independently to gp120 and the carboxy-terminal gp41 ectodomain alpha-helix to modulate changes in envelope protein conformation, which is involved in the fusion process. It is also possible that any relationship for a gp41 binding site in gp120 is indirect. Studies that seek to determine whether specific residues in the LZ interact with the putative gp41 binding site in gp120 to determine the gp120-gp41 dissociation phenotype may further clarify these possibilities.

The mechanisms of resistance of primary strains of HIV-1 to neutralization are of interest with regard to the potential for development of a vaccine effective in prevention of new infections. The availability of such a vaccine would be a powerful weapon in the effort to prevent the spread of HIV-1 infections. The results reported here demonstrate that this neutralization resistance can be mediated by effects of numerous nonepitope mutations in gp120 and gp41 that alter functional relationships among different regions of the envelope complex. Studies are ongoing in our laboratory to evaluate the role of mutations in and around the CD4 binding site, on the nonneutralizing face of the gp120 outer domain, and in the V1/V2 and V3 loop structures in determining neutralization resistance. The results of these studies to date are completely consistent with the hypothesis that we present based on the results described here, that concerted effects of interactions between different regions of the envelope determine the neutralization resistance, high-infectivity phenotype. To the extent that neutralization resistance of primary envelopes represents evolution of different envelopes toward a high-efficiency, conserved structure, rather than endless mutation of neutralization epitopes, it is likely that conserved, probably conformation-dependent epitopes will characterize primary HIV-1 envelopes. If so, the related challenge to vaccine design will be to construct immunogens that induce neutralizing antibody responses against these epitopes. The evidence that broadly cross-reactive, primary virus-neutralizing antibody responses may occur in HIV-1-infected people lends hope that such a goal may be feasible (41, 45, 46).

ACKNOWLEDGMENTS

This work was supported in part by National Institutes of Health grant AI 37438.

We thank Mike Flora at the Biomedical Instrumentation Center, USUHS, for gene sequencing and Cara Olson at the Biostatistics Consulting Center, USUHS, for statistical advice. We are indebted to John Sullivan, University of Massachusetts, for providing the primary MN virus used in this study.

REFERENCES

1. **Alkhatib, G., C. Combadiere, C. C. Broder, Y. Feng, P. E. Kennedy, P. M. Murphy, and E. A. Berger.** 1996. CC CKR5: a RANTES, MIP-1α, MIP-1β receptor as a fusion cofactor for macrophage-tropic HIV-1. Science **272:** 1955–1958.
2. **Back, N. K., L. Smit, J. J. De Jong, W. Keulen, M. Schutten, J. Goudsmit, and M. Tersmette.** 1994. An N-glycan within the human immunodeficiency virus type 1 gp120 V3 loop affects virus neutralization. Virology **199:**431–438.
3. **Berman, P. W., A. M. Gray, T. Wrin, J. C. Vennari, D. J. Eastman, G. R. Nakamura, D. P. Francis, G. Gorse, and D. H. Schwartz.** 1997. Genetic and immunologic characterization of viruses infecting MN-rgp120-vaccinated volunteers. J. Infect. Dis. **176:**384–397.
4. **Chan, D. C., D. Fass, J. M. Berger, and P. S. Kim.** 1997. Core structure of gp41 from the HIV envelope glycoprotein. Cell **89:**263–273.
5. **Connor, R. I., K. E. Sheridan, C. Lai, L. Zhang, and D. D. Ho.** 1996. Characterization of the functional properties of *env* genes from long-term survivors of human immunodeficiency virus type 1 infection. J. Virol. **70:** 5306–5311.
6. **Deng, H., R. Liu, W. Ellmeier, S. Choe, D. Unutmaz, M. Burkhart, P. Di Marzio, S. Marmon, R. E. Sutton, C. M. Hill, C. B. Davis, S. C. Peiper, T. J. Schall, D. R. Littman, and N. R. Landau.** 1996. Identification of a major co-receptor for primary isolates of HIV-1. Nature **381:**661–666.
7. **Edwards, T. G., S. Wyss, J. D. Reeves, S. Zolla-Pazner, J. A. Hoxie, R. W. Doms, and F. Baribaud.** 2002. Truncation of the cytoplasmic domain induces exposure of conserved regions in the ectodomain of human immunodeficiency virus type 1 envelope protein. J. Virol. **76:**2683–2691.
8. **Eiden, L. E., and J. D. Lifson.** 1992. HIV interactions with CD4: a continuum of conformations and consequences. Immunol. Today **13:**201–206.
9. **Feng, Y., C. C. Broder, P. E. Kennedy, and E. A. Berger.** 1996. HIV-1 entry cofactor: functional cDNA cloning of a seven-transmembrane, G protein-coupled receptor. Science **272:**872–877.
10. **Fouts, T. R., J. M. Binley, A. Trkola, J. E. Robinson, and J. P. Moore.** 1997.

Neutralization of the human immunodeficiency virus type 1 primary isolate JR-FL by human monoclonal antibodies correlates with antibody binding to the oligomeric form of the envelope glycoprotein complex. J. Virol. **71:**2779–2785.

11. **Gelderblom, H. R., E. H. Hausmann, M. Ozel, G. Pauli, and M. A. Koch.** 1987. Fine structure of human immunodeficiency virus (HIV) and immunolocalization of structural proteins. Virology **156:**171–176.
12. **Gurgo, C., H. G. Guo, G. Franchini, A. Aldovini, E. Collalti, K. Farrell, F. Wong-Staal, R. C. Gallo, and M. S. Reitz, Jr.** 1988. Envelope sequences of two new United States HIV-1 isolates. Virology **164:**531–536.
13. **Helseth, E., U. Olshevsky, C. Furman, and J. Sodroski.** 1991. Human immunodeficiency virus type 1 gp120 envelope glycoprotein regions important for association with the gp41 transmembrane glycoprotein. J. Virol. **65:**2119–2123.
14. **Ho, D. D., T. Moudgil, and M. Alam.** 1989. Quantitation of human immunodeficiency virus type 1 in the blood of infected persons. N. Engl. J. Med. **321:**1621–1625.
15. **Ivey-Hoyle, M., R. K. Clark, and M. Rosenberg.** 1991. The N-terminal 31 amino acids of human immunodeficiency virus type 1 envelope protein gp120 contain a potential gp41 contact site. J. Virol. **65:**2682–2685.
16. **Kalyanaraman, V. S., V. Rodriguez, F. Veronese, R. Rahman, P. Lusso, A. L. DeVico, T. Copeland, S. Oroszlan, R. C. Gallo, and M. G. Sarngadharan.** 1990. Characterization of the secreted, native gp120 and gp160 of the human immunodeficiency virus type 1. AIDS Res. Hum. Retrovir. **6:**371–380.
17. **Kang, C.-Y., K. Hariharan, P. L. Nara, J. Sodroski, and J. P. Moore.** 1994. Immunization with a soluble CD4-gp120 complex preferentially induces neutralizing anti-human immunodeficiency virus type 1 antibodies directed to conformation-dependent epitopes of gp120. J. Virol. **68:**5854–5862.
18. **Katzenstein, D. A., L. K. Vujcic, A. Latif, R. Boulos, N. A. Halsey, T. C. Quinn, S. C. Rastogi, and G. V. Quinnan, Jr.** 1990. Human immunodeficiency virus neutralizing antibodies in sera from North Americans and Africans. J. Acquir. Immune Defic. Syndr. **3:**810–816.
19. **Konno, S., and H. Yamamoto.** 1970. Pathology of equine infectious anemia. Proposed classification of pathological types of disease. Cornell Vet. **60:**393–449.
20. **Kowalski, M., J. Potz, L. Basiripour, T. Dorfman, W. C. Goh, E. Terwilliger, A. Dayton, C. Rosen, W. Haseltine, and J. Sodroski.** 1987. Functional regions of the envelope glycoprotein of human immunodeficiency virus type 1. Science **237:**1351–1355.
21. **Kwong, P. D., R. Wyatt, J. Robinson, R. W. Sweet, J. Sodroski, and W. A. Hendrickson.** 1998. Structure of an HIV gp120 envelope glycoprotein in complex with the CD4 receptor and a neutralizing human antibody. Nature **393:**630–631.
22. **Kwong, P. D., R. Wyatt, Q. J. Sattentau, J. Sodroski, and W. A. Hendrickson.** 2000. Oligomeric modeling and electrostatic analysis of the gp120 envelope glycoprotein of human immunodeficiency virus. J. Virol. **74:**1961–1972.
23. **Laman, J. D., M. M. Schellekens, Y. H. Abacioglu, G. K. Lewis, M. Tersmette, R. A. Fouchier, J. P. Langedijk, E. Claasen, and W. J. Boersma.** 1992. Variant-specific monoclonal and group-specific polyclonal human immunodeficiency virus type 1 neutralizing antibodies raised with synthetic peptides from the gp120 third variable domain. J. Virol. **66:**1823–1831.
24. **Matsushita, S., M. Robert-Guroff, J. Rusche, A. Koito, T. Hattori, H. Hoshino, K. Javaherian, K. Takatsuki, and S. Putney.** 1988. Characterization of a human immunodeficiency virus neutralizing monoclonal antibody and mapping of the neutralizing epitope. J. Virol. **62:**2107–2114.
25. **McCune, J. M., L. B. Rabin, M. B. Feinberg, M. Lieberman, J. C. Kosek, G. R. Reyes, and I. L. Weissman.** 1988. Endoproteolytic cleavage of gp160 is required for the activation of human immunodeficiency virus. Cell **53:**55–67.
26. **McKeating, J. A., J. Cordell, C. J. Dean, and P. Balfe.** 1992. Synergistic interaction between ligands binding to the CD4 binding site and V3 domain of human immunodeficiency virus type I gp120. Virology **191:**732–742.
27. **McKnight, A., and P. R. Clapham.** 1995. Immune escape and tropism of HIV. Trends Microbiol. **3:**356–361.
28. **Montefiori, D. C., G. Pantaleo, L. M. Fink, J. T. Zhou, J. Y. Zhou, M. Bilska, G. D. Miralles, and A. S. Fauci.** 1996. Neutralizing and infection-enhancing antibody responses to human immunodeficiency virus type 1 in long-term nonprogressors. J. Infect. Dis. **173:**60–67.
29. **Moore, J. P., J. A. McKeating, Y. X. Huang, A. Ashkenazi, and D. D. Ho.** 1992. Virions of primary human immunodeficiency virus type 1 isolates resistant to soluble CD4 (sCD4) neutralization differ in sCD4 binding and glycoprotein gp120 retention from sCD4-sensitive isolates. J. Virol. **66:**235–243.
30. **Moore, J. P., J. A. McKeating, W. A. Norton, and Q. J. Sattentau.** 1991. Direct measurement of soluble CD4 binding to human immunodeficiency virus type 1 virions: gp120 dissociation and its implications for virus-cell binding and fusion reactions and their neutralization by soluble CD4. J. Virol. **65:**1133–1140.
31. **Moore, J. P., J. A. McKeating, R. A. Weiss, and Q. J. Sattentau.** 1990. Dissociation of gp120 from HIV-1 virions induced by soluble CD4. Science **250:**1139–1142.
32. **Nara, P. L., L. Smit, N. Dunlop, W. Hatch, M. Merges, D. Waters, J. Kelliher, R. C. Gallo, P. J. Fischinger, and J. Goudsmit.** 1990. Emergence of viruses resistant to neutralization by V3-specific antibodies in experimental human immunodeficiency virus type 1 IIIB infection of chimpanzees. J. Virol. **64:**3779–3791.
33. **Park, E. J., M. K. Gorny, S. Zolla-Pazner, and G. V. Quinnan, Jr.** 2000. A global neutralization resistance phenotype of human immunodeficiency virus type 1 is determined by distinct mechanisms mediating enhanced infectivity and conformational change of the envelope complex. J. Virol. **74:**4183–4191.
34. **Park, E. J., and G. V. Quinnan, Jr.** 1999. Both neutralization resistance and high infectivity phenotypes are caused by mutations of interacting residues in the human immunodeficiency virus type 1 gp41 leucine zipper and the gp120 receptor- and coreceptor-binding domains. J. Virol. **73:**5707–5713.
35. **Park, E. J., L. K. Vujcic, R. Anand, T. S. Theodore, and G. V. Quinnan, Jr.** 1998. Mutations in both gp120 and gp41 are responsible for the broad neutralization resistance of variant human immunodeficiency virus type 1 MN to antibodies directed at V3 and non-V3 epitopes. J. Virol. **72:**7099–7107.
36. **Perelson, A. S., A. U. Neumann, M. Markowitz, J. M. Leonard, and D. D. Ho.** 1996. HIV-1 dynamics in vivo: virion clearance rate, infected cell life-span, and viral generation time. Science **271:**1582–1586.
37. **Reitz, M. S., Jr., C. Wilson, C. Naugle, R. C. Gallo, and M. Robert-Guroff.** 1988. Generation of a neutralization-resistant variant of HIV-1 is due to selection for a point mutation in the envelope gene. Cell **54:**57–63.
38. **Sawyer, L. A., D. A. Katzenstein, R. M. Hendry, E. J. Boone, L. K. Vujcic, C. C. Williams, S. L. Zeger, A. J. Saah, C. R. Rinaldo, Jr., J. P. Phair, et al.** 1990. Possible beneficial effects of neutralizing antibodies and antibody-dependent, cell-mediated cytotoxicity in human immunodeficiency virus infection. AIDS Res. Hum. Retrovir. **6:**341–356.
39. **Sullivan, N., Y. Sun, Q. Sattentau, M. Thali, D. Wu, G. Denisova, J. Gershoni, J. Robinson, J. Moore, and J. Sodroski.** 1998. CD4-induced conformational changes in the human immunodeficiency virus type 1 gp120 glycoprotein: consequences for virus entry and neutralization. J. Virol. **72**:4694–4703.
40. **Thali, M., J. P. Moore, C. Furman, M. Charles, D. D. Ho, J. Robinson, and J. Sodroski.** 1993. Characterization of conserved human immunodeficiency virus type 1 gp120 neutralization epitopes exposed upon gp120-CD4 binding. J. Virol. **67:**3978–3988.
41. **Vujcic, L. K., and G. V. Quinnan, Jr.** 1995. Preparation and characterization of human HIV type 1 neutralizing reference sera. AIDS Res. Hum. Retrovir. **11:**783–787.
42. **Weissenhorn, W., A. Dessen, S. C. Harrison, J. J. Skehel, and D. C. Wiley.** 1997. Atomic structure of the ectodomain from HIV-1 gp41. Nature **387:**426–430.
43. **Wyatt, R., P. D. Kwong, E. Desjardins, R. W. Sweet, J. Robinson, W. A. Hendrickson, and J. G. Sodroski.** 1998. The antigenic structure of the HIV gp120 envelope glycoprotein. Nature **393:**705–711.
44. **Wyatt, R., N. Sullivan, M. Thali, H. Repke, D. Ho, J. Robinson, M. Posner, and J. Sodroski.** 1993. Functional and immunologic characterization of human immunodeficiency virus type 1 envelope glycoproteins containing deletions of the major variable regions. J. Virol. **67:**4557–4565.
45. **Zhang, P. F., P. Bouma, E. J. Park, J. B. Margolick, J. E. Robinson, S. Zolla-Pazner, M. N. Flora, and G. V. Quinnan, Jr.** 2002. A variable region 3 (V3) mutation determines a global neutralization phenotype and CD4-independent infectivity of a human immunodeficiency virus type 1 envelope associated with a broadly cross-reactive, primary virus-neutralizing antibody response. J. Virol. **76:**644–655.
46. **Zhang, P. F., X. Chen, D. W. Fu, J. B. Margolick, and G. V. Quinnan, Jr.** 1999. Primary virus envelope cross-reactivity of the broadening neutralizing antibody response during early chronic human immunodeficiency virus type 1 infection. J. Virol. **73:**5225–5230.
47. **Zhang, W., A. P. Godillot, R. Wyatt, J. Sodroski, and I. Chaiken.** 2001. Antibody 17b binding at the coreceptor site weakens the kinetics of the interaction of envelope glycoprotein gp120 with CD4. Biochemistry **40:**1662–1670.